Novel Power Control of Voltage-Controlled Inverters for Grid Inertia Support

Xiangjun Quan
School of Electrical Engineering
Southeast University
University of Texas at Austin
NanJing, China
qxj@seu.edu.cn

Xin Zhao
Department of Electrical and Computer Engineering
University of Texas at Austin
Austin, USA
xin.zhao@utexas.edu

Liqi Zhang
Department of Electrical and Computer Engineering
University of Texas at Austin
Austin, USA
liqi.zhang@utexas.edu

Rong Xu
Department of Electrical and Computer Engineering
University of Texas at Austin
Austin, USA
rxu@utexas.edu

Yang Lei
Department of Electrical and Computer Engineering
University of Texas at Austin
Austin, USA
ylei@utexas.edu

Alex Q. Huang
Department of Electrical and Computer Engineering
University of Texas at Austin
Austin, USA
aqhuang@utexas.edu

***Abstract*—Nowadays, the voltage-controlled inverter for grid-connected application has been paid great attentions due to its advantages. The power control is important for the voltage-controlled grit-tied inverter to realize advanced function, such as the droop control or virtual-synchronous-generator control. For the power control purpose, this paper proposed a design method for the inertia support control. Compared with the conventional power control, the inertia time and the power amplitude can be customized when grid frequency changes. The detailed design method is provided and verified by the experiment results.**

Keywords—component, formatting, style, styling, insert (*key words****)***

I. INTRODUCTION

As the interface between the distributed generation (DG) and the grid, the grid-connected inverter can be classified as current-controlled (CC) or voltage-controlled (VC) [1]. The CC inverter has been widely used for DG applications due to its advantages of fast dynamics and well developed knowledge base. However, nowadays, the VC inverter, due to its attractive merit of voltage source characteristic, has been attracted more interests than the conventional current-controlled (CC) inverter [2].

Based on a well-tuned inner voltage control loop, the key feature of the voltage-controlled inverter is the inherent power control capability when connected to the grid or other VC inverters. The most popular power control methods are the droop control [3]-[9] and virtual synchronous generator (VSG) control [10]-[14]. Furthermore, it is indicated in [15] that they are basically equivalent, but the designed control parameters have different physical meanings.

For droop control, its fundamental functionalities are power sharing and grid support. The conventional droop controls can be further classified into active power-phase (P-δ) control [5], [6], active power-frequency (P-ω) control [7], [8] and reactive power-voltage (Q-V) control. On the other hand the VSG control is to mimic the characteristics of a synchronous generator. It leads to the same inertia equation between the active power and frequency as long as the related parameters satisfy a certain relationship [15]. When considering the closed-loop control for the active power, the dynamic performance of the droop control and VSG control is typically not satisfactory, since the parameters are designed by interpreting physical meanings, such as inertia time and power sharing gain. Many techniques are proposed to improve the dynamic response of the power control for the VC inverter. The proportional-differentiation (PD) controller is proposed for droop control in [7], [8]. For VSG control, a detailed small signal analysis is introduced in [11]. The step-by-step parameter design guideline is also illustrated to acquire a good dynamic response for VSG power control. However, the inertia time constant of the power loop is not adjustable, because the parameters are selected to guarantee a good dynamic performance. In [12], a method to directly regulate desired transient and steady-state behavior is proposed by introducing a damping correction loop. However this approach makes the control complicated.

Moreover, depending on energy storage size and configurations, the applications are divided into two types: one is for the inertia support [13], and the other one is for the primary frequency regulation (droop control) [14]. The inertia support needs to output active power for a short period of time, defined as inertia time, when the grid frequency changes. While the droop control requires a longer time active power support for the grid when the grid frequency changes. For the inertia support control, it is desirable that the inertia time and the maximum power amplitude during the dynamic process are adjustable. This is not an easy task while still maintaining a good dynamic performance. This paper focuses on a novel inertia support control for the VC inverter with improved performance.

To develop an inertia-support power control loop which has adjustable inertia time and maximum power amplitude during the power dynamic, this paper utilizes the frequency and phase as the control variables simultaneously, resulting in a second-order system for the active power control. Then a reference feedforward is introduced to cancel a pole of the system, so that the power tracking system becomes a first-order system. Consequently, the inertia time can be defined by another pole, and the power amplitude can be determined be the cancelled pole without affecting the dynamic performance of the VC inerter.

II. Power Control for Inertia Support

The application topology of the VC inverter is shown in Fig. 1 where a PV or a load is paralleled with the VC inverter with an energy storage unit connected to the DC side. The VC inverter and PV (or load) are all connected to the grid with an inductor (including the line impedance). The active and reactive power can be controlled by means of changing the frequency or phase and amplitude of the VC inverter voltage. The detailed mathematical model of the power control is illustrated in [11]. To clarify the proposed power control, the mathematical models governing p and q are expressed in (1):

$$\begin{cases} p = \dfrac{U_C U_g \sin(\Delta\delta)}{X} \approx \dfrac{U_C U_g \Delta\delta}{X} = A\Delta\delta \\ q = \dfrac{U_C^2 - U_C U_g \cos(\Delta\delta)}{X} \approx \dfrac{U_C (U_C - U_g)}{X} = B\Delta U \end{cases} \quad (1)$$

where $\Delta\delta$ denotes the phase difference, ΔU is the amplitude difference between the inverter and grid.

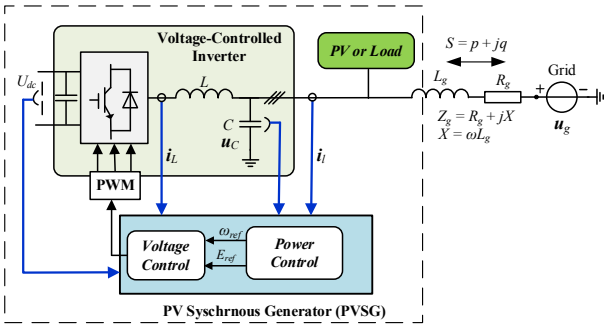

Fig. 1. Topology of the grid-connected voltage-controlled inverter. The overall system can be referred as a PV Sychrnous Generator (PVSG)

A. Power Control Design

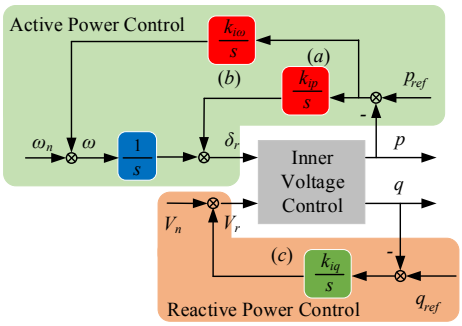

Fig. 2. Proposed power control

Based on (1), a power control strategy of inertia support is designed as shown in Fig. 2 where the frequency and phase are both used as the control variable to regulate the active power. The controller (b) is used to automatically synchronize to the grid which is necessary for mimicking the characteristic of a synchronous generator. Compared with the conventional droop control, the controller (a) is introduced in the proposed control to damp the system, since the proportional droop control, which also plays the role of damping, is absent in the inertia support control. The controller (c) performs the reactive power control. Since this paper mainly focuses on the active power inertia control, the reactive power control is not discussed. The detailed reactive power droop control is discussed in [11].

B. Inertia Support for PV Plant

For the application shown in Fig. 1, as long as the conventional PV with P/Q control is connected to the terminal of the VC inverter with proposed control, the conventional PV will be automatically modified to the output characteristic of a synchronous generator, here the overall system can be referred as PV synchronous generator (PVSG). The fluctuation power of the PV is automatically filtered by the VC inverter. At the instant when the PV power changes, the power flow between the VC inverter and the grid remains invariable (the voltage imposed at the two point of the line is not changed), so that the step power change from the PV has to flow into the VC inverter, then after a while (this time depends on the control parameters), the power will be forced to its reference due to the controller (a) and (b), which means that the step power change in PV will flow into the grid slowly. Consequently, the power filter function is achieved automatically to avoid the impulse power flowing into grid directly.

III. Parameter Design

According to the proposed control shown in Fig. 2 and the model of (1), the closed-loop control of active power can be described by the block diagram shown in Fig. 3. To stabilize the system, k_{ip} is introduced and $k_{i\omega}$ is used to realize the zero-static-state-error control. The parameter k_r is adopted to tune the performance of the power tracking control. The closed-loop transfer function is therefore

$$\begin{aligned} p &= G_{rp}(s)\, p_{ref} + G_{\omega p}(s)\, \Delta\omega_g \\ &= \frac{A(k_{ip} + k_r)s + Ak_{i\omega}}{s^2 + Ak_{ip}s + Ak_{i\omega}} p_{ref} + \frac{As}{s^2 + Ak_{ip}s + Ak_{i\omega}} \Delta\omega_g \end{aligned} \quad (2)$$

where $\Delta\omega_g = \omega_n - \omega_g$. As can be seen in (2), with the absence of a droop coefficient, the introduction of k_{ip} can damp the system to make the system stable. The tracking performance is depended on the transfer function $G_{rp}(s)$, while the power response when the grid frequency changes is determined by $G_{\omega p}(s)$. Hence the power control is actually to shape $G_{rp}(s)$ and $G_{\omega p}(s)$.

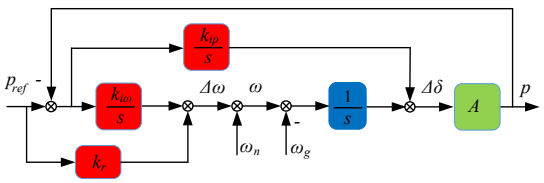

Fig. 3. Proposed active power control

For the power control of inertia support, there are two specifications that need to be satisfied. The first one is that the settling time of the tracking control should be adjustable (actually this time is also the inertia time), this part is achieved by the design of the closed-loop poles of the system. Second, the maximum power amplitude of the power

response when grid frequency changes should be designable. This index depends on the amplitude response of $G_{\omega p}(s)$. To achieve this two specifications, (2) is rewritten in zero-pole formation:

$$p = \frac{A\left(k_{ip}+k_r\right)\left(s+z\right)}{\left(s+p_1\right)\left(s+p_2\right)} p_{ref} + \frac{As}{\left(s+p_1\right)\left(s+p_2\right)} \Delta\omega_g \quad (3)$$

Then, it has the relationship between the control parameters and zeros and poles:

$$Ak_{ip} = p_1 + p_2\,, \quad Ak_{i\omega} = p_1 p_2\,, \quad z = \frac{k_{i\omega}}{k_{ip}+k_r} \quad (4)$$

If command $z = p_2$, the reference-to-power transfer function becomes

$$G_{rp}\left(s\right) = \frac{A\left(k_{ip}+k_r\right)}{s+p_1} = \frac{p_1}{s+p_1} \quad (5)$$

which implies that the power tracking control becomes a first-order system, so that it has a good dynamic performance like a first-order system and its time constant can be adjusted by p_1.

Furthermore, maximum power amplitude in the transient process is not only related with the maximum current that flows through the equipment, but also determines the energies required during the dynamic-support duration. Hence, to flexibly design the maximum power amplitude in the transient process when the grid frequency changes, $G_{\omega p}(s)$ is rewritten as

$$G_{\omega p}\left(j\omega\right) = \frac{Aj\omega}{-\omega^2 + \left(p_1+p_2\right)j\omega + p_1 p_2} \quad (6)$$

By computing derivation of (6) with respect of frequency ω, the maximum amplitude of (6) can be determined as:

$$\left|G_{\omega p}\left(j\omega\right)\right|_{\max} = \frac{A}{p_1+p_2} \quad (7)$$

when $\omega = \sqrt{p_1 p_2}$. This value is actually the maximum power during the dynamic response when the grid frequency changes. Correspondingly, the power amplitude can be tuned by the placement of p_2 without affecting the power tracking performance, because this pole is cancelled by the zero.

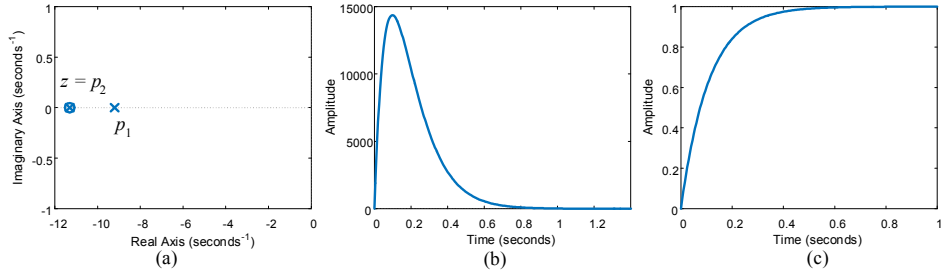

Fig. 4. Design result T_{Aset} = 0.5s, ΔP = 15kW: (a) zero-pole location; (b) step response of $G_{\omega p}(s)$; (c) step response of $G_{rp}(s)$

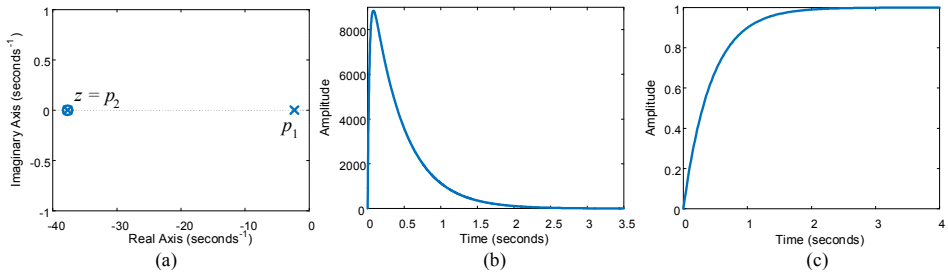

Fig. 5. Design result T_{Aset} = 2s, ΔP = 10kW: (a) zero-pole location; (b) step response of $G_{\omega p}(s)$; (c) step response of $G_{rp}(s)$

To summary, the design process for the proposed control is:

1) determine the settling time of the power control T_{Aset} and the maximum power amplitude ΔP when grid frequency changes 1 Hz;

2) compute the location of poles by: $p_1 = 4.6/T_{Aset}$, $p_2 = 2\pi A/\Delta P - p_1$;

3) determine the control parameters according to (4):

$$k_{ip} = \frac{p_1+p_2}{A}, \quad k_{i\omega} = \frac{p_1 p_2}{A}, \quad k_r = \frac{k_{i\omega}}{p_2} - k_{ip} \quad (8)$$

Following the proposed design process 1)-3), two example controls are designed to demonstrate different performance for a system with $U_C = U_g$ = 170 V, L_g = 1.8 mH，$\omega_g = 120\pi$, X = 0.67854 Ω. Fig. 4 shows the design of T_{Aset} = 0.5s, ΔP = 15kW. While in Fig. 5, the designed parameters result in T_{Aset} = 2s, ΔP = 10kW. As shown in Fig. 4 and Fig. 5, the pole p_2 and z are overlapped, and the settling time is determined by p_1. The step responses of $G_{\omega p}(s)$ for different designs are shown in Fig. 4 (b) and Fig. 5 (b). $G_{\omega p}(s)$ represents the performance of grid frequency change. As can be observed in Fig. 4 (b) and Fig. 5 (b), the achieved maximum power amplitudes are consistent with the designed value of 15 kW and 10 kW respectively. For the tracking control performance, the step response of $G_{rp}(s)$ with different settling-time designs are shown in Fig. 4 (c) and Fig. 5 (c). From Fig. 4 (c) and Fig. 5 (c), the settling times are 0.5 s and 2 s which are the designed values. Therefore the simulation validate the proposed control.

IV. Experiment Results

To verify the proposed power control algorithm, two comparison experiments are conducted. In the experiment setup, a supercapacitor with a capacitance of 3 F is connected at the DC side to supply the real physical inertia and maintain the DC voltage for the inverter. The tested system parameters are the same with the one in the design section. The results are shown in Fig. 6 and Fig. 7.

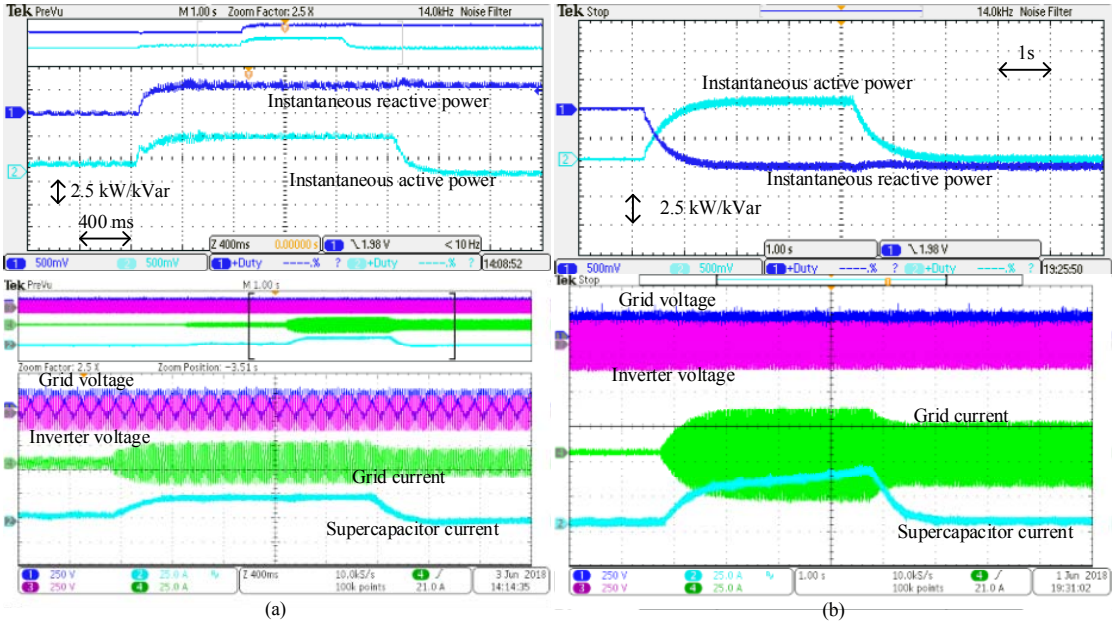

(a) (b)

Fig. 6. Experiment results for reference step: (a) T_{Aset} = 0.5s; (b) T_{Aset} = 2s

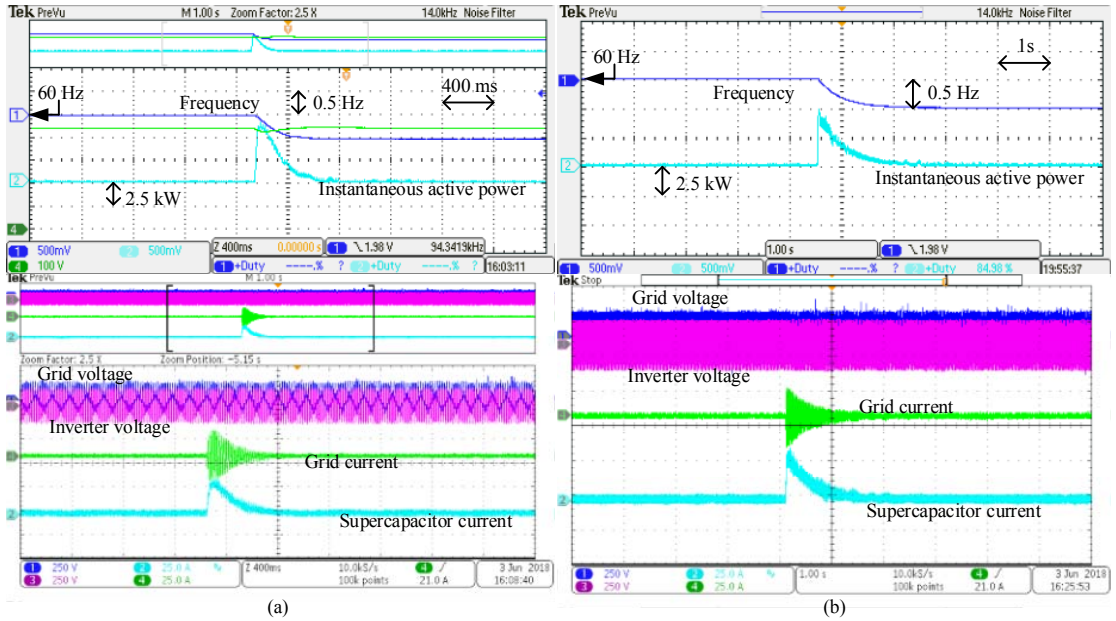

(a) (b)

Fig. 7. Experiment results for grid frequency change: (a) T_{Aset} = 0.5s, ΔP = 15kW; (b) T_{Aset} = 2s, ΔP = 10kW

Fig. 6 shows the performance of the reference step with different settling time. As in Fig. 6 (a), the settling time is designed as 0.5 s, when the active power reference stepped from 2 kW to 5 kW then came back to zero, the active power can track the power reference perfectly with a good dynamic response and achieve its steady state in 0.5 s which is conformed to the design target. The current of the supercapacitor (blue line) also represents the active power output which verifies the effectiveness of the proposed method. While in Fig. 6 (b), the active power reference changed from zero to 5 kW and the settling time is designed as 2s, the active power response shows that the zero-static-state-error active power control is achieved with the settling time of 2 s, and the dynamic response is also very good due to the first-order system behaviors of the VC inverter.

In Fig. 7, the response of grid frequency change for 0.5s-15kW/Hz and 2s-10kW/Hz designs are shown. Fig. 7 (a)

shows that when grid frequency decreased 0.5 Hz, the inverter outputted an active power immediately to provide the inertia support. The maximum power is approximate 7.5 kW during the dynamic process and the transient time is 0.5 s, the frequency of the inverter also automatically synchronized to the grid in 0.5 s. The results prove that the predefined specifications are achieved and the proposed control is verified. For the 2s-10kW/Hz design, its response to grid frequency step is displayed in Fig. 7 (b). As shown in Fig. 7 (b), when grid frequency steps -0.5 Hz, the inverter generated a maximum power injection of 5 kW. The dynamic time for the synchronization and output power is 2 s which is the designed inertia time. The effectiveness of the proposed method is proven. Moreover, it is worth noting that, for the larger inertia time, the energy fed into grid when frequency changes is bigger which means that more energy stored in the supercapacitor is needed. Hence the customized inertia time is meaningful for different storage applications.

V. Conclusions and Future Work

A novel inertia support power control is proposed in this paper for the voltage-controlled inverter. Thanks to the proposed novel control approach, the inertia time and the maximum power amplitude during the dynamic-support process can be designed independently to satisfy different application requirements with different storage configurations. The power tracking control is reduced to a first-order system, so that the power control loop has a good dynamic performance with customized settling time and zero overshoot. At last the experiment results verify the correctness and effectiveness of the proposed method.

Acknowledgment

This work is partially supported by Duke Energy. We would like to thank Tianxiang Chen and Ruiyang Yu for the work of the control board sincerely.

References

[1] J. Rocabert, A. Luna, F. Blaabjerg and P. Rodríguez, "Control of Power Converters in AC Microgrids," *IEEE Trans. Power Electron*, vol. 27, no. 11, pp. 4734-4749, Nov. 2012.

[2] P. Piya, M. Ebrahimi, M. Karimi-Ghartemani and S. A. Khajehoddin, "Fault Ride-Through Capability of Voltage-Controlled Inverters," in *IEEE Transactions on Industrial Electronics*, vol. 65, no. 10, pp. 7933-7943, Oct. 2018.

[3] Y. Deng, Y. Tao, G. Chen, G. Li and X. He, "Enhanced Power Flow Control for Grid-Connected Droop-Controlled Inverters With Improved Stability," in IEEE Transactions on Industrial Electronics, vol. 64, no. 7, pp. 5919-5929, July 2017.

[4] J. M. Guerrero, J. C. Vasquez, J. Matas, L. G. de Vicuna and M. Castilla, "Hierarchical control of droop-controlled AC and DC microgrids—a general approach toward standardization," *IEEE Trans. Industrial Electron*., vol. 58, no. 1, pp. 158-172, Jan. 2011.

[5] Guerrero, J. M., De Vicuna, L. G., Matas, J., Castilla, M., & Miret, J. . "A wireless controller to enhance dynamic performance of parallel inverters in distributed generation systems". *IEEE Trans. Power Electron*., vol.19, no.5, pp.1205-1213, Sep. 2004.

[6] J. C. Vasquez, J. M. Guerrero, M. Savaghebi, J. Eloy-Garcia and R. Teodorescu, "Modeling, Analysis, and Design of Stationary-Reference-Frame Droop-Controlled Parallel Three-Phase Voltage Source Inverters," in *IEEE Transactions on Industrial Electronics*, vol. 60, no. 4, pp. 1271-1280, April 2013.

[7] J. M. Guerrero, J. C. Vasquez, J. Matas, M. Castilla and L. Garcia de Vicuna, "Control strategy for flexible microgrid based on parallel line-interactive UPS systems," IEEE Trans. Industrial Electron., vol. 56, no. 3, pp. 726-736, Mar. 2009.

[8] Y. A. R. I. Mohamed and E. F. El-Saadany, "Adaptive Decentralized Droop Controller to Preserve Power Sharing Stability of Paralleled Inverters in Distributed Generation Microgrids," IEEE Trans. Power Electron., vol. 23, no. 6, pp. 2806-2816, Nov. 2008.

[9] Y. Sun, X. Hou, J. Yang, H. Han, M. Su and J. M. Guerrero, "New Perspectives on Droop Control in AC Microgrid," in IEEE Transactions on Industrial Electronics, vol. 64, no. 7, pp. 5741-5745, July 2017.

[10] Q. C. Zhong and G. Weiss, "Synchronverters: Inverters That Mimic Synchronous Generators," in IEEE Transactions on Industrial Electronics, vol. 58, no. 4, pp. 1259-1267, April 2011.

[11] H. Wu et al., "Small-Signal Modeling and Parameters Design for Virtual Synchronous Generators," in IEEE Transactions on Industrial Electronics, vol. 63, no. 7, pp. 4292-4303, July 2016.

[12] S. Dong and Y. C. Chen, "A Method to Directly Compute Synchronverter Parameters for Desired Dynamic Response," in *IEEE Transactions on Energy Conversion*, vol. 33, no. 2, pp. 814-825, June 2018.

[13] D. Chen, Y. Xu and A. Q. Huang, "Integration of DC Microgrids as Virtual Synchronous Machines Into the AC Grid," in IEEE Transactions on Industrial Electronics, vol. 64, no. 9, pp. 7455-7466, Sept. 2017.

[14] J. Fang, Y. Tang, H. Li and X. Li, "A Battery/Ultracapacitor Hybrid Energy Storage System for Implementing the Power Management of Virtual Synchronous Generators," in IEEE Transactions on Power Electronics, vol. 33, no. 4, pp. 2820-2824, April 2018.

[15] S. D'Arco and J. A. Suul, "Equivalence of virtual synchronous machines and frequency-droops for converter-based microgrids,"IEEETrans. Smart Grid, vol. 5, no. 1, pp. 394–395, Jan. 2014.